More-Than-Topology-Preserving Flows for Active Contours and Polygons

Ganesh Sundaramoorthi and Anthony Yezzi
School of Electrical and Computer Engineering
Georgia Institute of Technology
Atlanta, GA 30332
{ganeshs, ayezzi}@ece.gatech.edu

Abstract

Active contour and active polygon models have been used widely for image segmentation. In some applications, the topology of the object(s) to be detected from an image is known a priori, despite an unknown complex geometry, and it is important that the active contour or polygon maintain the desired topology. In this work, we construct a novel geometric flow that can be added to image based evolutions of active contours and polygons so that the topology of the initial contour or polygon is preserved. Indeed, the proposed geometric flow ensures more than just correct topology; it ensures that the active contour or polygon is, in some sense, kept far away from a topology change. Smoothness properties similar to curvature flow are also guaranteed by the proposed geometric flow. The proposed topology preserving geometric flow is the gradient flow arising from an energy that is based on electrostatic principles. The evolution of a single point on the contour depends on all other points of the contour, which is different from traditional curve evolutions in computer vision literature.

1. Introduction

Active contours (see for example [14, 3, 15, 23, 4, 19]) and active polygons [2, 22], have been used widely for image segmentation. Level set methods [18] for implementing active contours have been praised for their ability to handle topology changes. However in many applications, such as brain cortex segmentation [11], [9] and dendrite segmentation [12], the topology of the object(s) to be segmented is known *a priori*, and therefore there is a desire to maintain the known topology throughout an evolution. In this work, we derive a geometric flow that can be added to an existing image based curve or polygon evolution. The geometric flow is derived by minimizing an energy that is similar to the electrostatic potential energy of a curve or polygon with a uniform charge distributed along its perimeter. Our geometric flow is guaranteed to preserve the topology of the initial contour(s), while affecting the original image based evolution strongly when the curve becomes close to topology change. Note that although curvature flow keeps a curve, which is homeomorphic to the circle, embedded [7, 8], i.e., prevents topology change, this is not the case when curvature flow is combined with an image based term. Moreover for multiple curves evolving under curvature flow, the result of [7, 8] no longer holds.

Figure 1. Two circles (left), two circles with thin strip connecting them (right). The curves that are boundaries of these regions on the left and right have different topologies; however, the curves are "close".

Since topology is, in some sense, a weak property of a curve, it is useful in applications that the segmentation method does more than just ensure correct topology. To get a sense of what we mean by topology being a weak property, consider Fig. 1. The curves that are the boundaries of the regions illustrated in Fig. 1 have different topologies; however, they are in a certain sense very "close". For example, using the metric that is the Lebesgue measure of the set-symmetric difference of the regions enclosed by the contours, we can say that the curves in Fig. 1 are close. In fact, one can say that with respect to this metric, the set of curves with a fixed topology is a dense set in the set of all curves. Thus, it is possible by just preserving topology, to obtain a curve with correct topology but that looks close to a curve with the wrong topology. We add that our proposed flows go further than simply preserving topology. As the active contour or polygon moves closer to a topology change, there is an increasingly forceful term arising from our proposed flow that gradually and gracefully moves the curve away from topology change. This implies that the curve, in some sense, remains far from topology change.

Proceedings of the Tenth IEEE International Conference on Computer Vision (ICCV'05)
1550-5499/05 $20.00 © 2005 **IEEE**

We will make precise what is meant by close and far to a topology change in Section 3.2. As we shall see in experiments in Section 5, this property of our flow is particularly useful. Another important property of our flows is that it has smoothing properties similar to curvature flow; hence, a curve is kept smooth and a polygon is kept regular.

2. Related Work

A topology preserving level set method is formulated in the work of Han *et al.* [10]. In their work, the authors take advantage of the fact that the active contours they consider are evolving on a discrete grid, which is the domain of the level set function. The idea of Han's algorithm is to detect the grid points of the level set function that will change sign at each iteration of the level set function evolution. These grid points are the only locations where a topology change can occur. If a topology change will occur at one of these grid points as a result of updating the level set function, then the function value at this grid point is not changed. A condition for detecting topology change at a grid point is derived, which is based on the configuration of the level set function in a small neighborhood of the grid point. Although this method guarantees that the resulting segmentation has the correct topology, there are some undesirable features of this method. First, the method is highly dependent on the grid spacing of the level set function. Thus, choosing a different grid spacing will result in a different segmentation. Moreover, the authors state that different segmentations can result as a consequence of the specific order that grid points are visited. Next, the topology preservation is an abrupt, discontinuous motion that is unnatural. Often times, as we shall see in Section 5, one obtains an unnatural segmentation that is very close to self intersection, and is only separated by a minimal spacing that is determined by the grid spacing. Finally, topology preservation is restricted to evolutions that are implemented using level set methods. As we shall see, our geometric flow has none of these undesirable features.

Our work is motivated by the polygon regularizer developed in the work of Unal *et al.* [22]. Unal assumes that an active polygon has a uniform charge distributed along its perimeter. The polygon moves in response to the electrostatic force and an image based term. The electrostatic force at each vertex is infinite due to the near neighbor effects of the adjacent segments to a vertex. To deal with the numerical problems associated with the computation of the electrostatic force, the near neighbor effects are simply ignored. Although, this method works in some cases, there are cases when the method cannot prevent self intersection of the polygon. We have also observed that as the number of vertices of the polygon becomes large, approaching the continuum, the flow becomes unstable. Other works in computer vision that use electrostatic principles for image segmentation, but are not and cannot be used for topology preservation are [5], [13].

The energies we consider in this paper are similar to energies introduced in the mathematical literature on knot energies [17], [6]. These energies are modifications of the electrostatic potential energy. The purpose of knot energies in [17] is to identify the *knot type* of a knot; a knot is an embedding of the circle into $\mathbb{R}^3$. Gradient flows are not considered in these papers, and the particular energy we use, for a reason we will mention in Section 3.2, is not considered in knot energy literature.

Finally, we mention the work of Rochery *et al.* [20] that considers a general class of double integral energies on curves whose gradient flows are used to enforce prior shape knowledge. Although at a first glance it may appear that the energy we consider falls into the general class considered by Rochery, this is not the case. First, the integrand of our energy is not a simple function of Euclidean distance, which is the case for Rochery's energies. Second, there is a dot product of velocity vectors in the integrand of Rochery's energy that leads to "chaotic" behavior. In fact, it is this phenomena that makes the model of Rochery unsuitable for topology preservation.

3. Variational Approach

We shall first give a mathematical definition of the active polygons and active contours that we consider in this paper. Let the domain of the image we wish to segment with a polygon or contour be denoted $\mathcal{I}$, where $\mathcal{I} \subset \mathbb{R}^2$. An active n-polygon is a polygon with vertices $v_0, \ldots, v_{n-1}$, where $n \in \{3, 4, \ldots\}$, in $\mathcal{I}$ that move at each instant of time according to the set of ordinary differential equations

$$\frac{\mathrm{d}v_k}{\mathrm{d}t}(t) = I_k(t) + \alpha R_k(t), \text{where } k \in \mathbb{Z}_n \tag{1}$$

where $I_k, R_k : \mathbb{R}^+ \to \mathbb{R}^2$, $\mathbb{Z}_n = \{0, 1, \ldots, n-1\}$, and $\alpha \in \mathbb{R}^+$. I_k is the force derived from the image we wish to segment, and R_k is a regularizing and topology preserving force that is derived only from the geometry of the polygon. We assume continuity and uniform boundedness of I_k, that is,

$$\sup_{t \in \mathbb{R}^+, k=0,1,\ldots,n-1} \|I_k(t)\| < +\infty, \tag{2}$$

where $\| \cdot \|$ is the Euclidean norm of $\cdot$. An active contour C is a twice differentiable curve in $\mathcal{I}$ that moves at each instant of time according to the partial differential equation

$$\frac{\partial C}{\partial t}(p,t) = i(p,t)\mathcal{N}(p,t) + \alpha \mathcal{R}(p,t) \tag{3}$$

where $p \in [0,1]$ denotes a parametrization of the curve C, $i : [0,1] \times \mathbb{R}^+ \to \mathbb{R}$, and $\mathcal{R} : [0,1] \times \mathbb{R}^+ \to \mathbb{R}^2$. The image based force is the term $i\mathcal{N}$, where $\mathcal{N}$ is the unit normal vector to the curve C. The regularizing and topology

preserving term of the active contour is $\mathcal{R}$. We make the assumptions that i is continuous and uniformly bounded, i.e.,

$$\sup_{t\in\mathbb{R}^+,p\in[0,1]} |i(p,t)| < +\infty. \tag{4}$$

Note that our assumptions on I_k and i are not too restrictive, and are typically true in practical applications. For example, Mumford-Shah [16], Chan-Vese [4], and other region based curve evolutions satisfy these conditions.

Our approach to derive R_k and $\mathcal{R}$ to preserve the topology of the initial configurations is to minimize an energy. The resulting gradient of this energy will correspond to R_k and $\mathcal{R}$. The gradient of the proposed energy approaches infinity as the curve approaches self intersection, and becomes large when the curve is "irregular". The intuition for our approach is from electrostatics. We imagine that the curve has a uniformly distributed charge along its perimeter, and that the curve moves in response to the charge as well as its original image based force. We expect that as the curve becomes close to self intersection, a repulsive force will arise due to its charge distribution and prevent self intersection. With this intuition, we propose the energy functional

$$E_\infty(C) = \frac{1}{2}\iint_{C\times C} \frac{\mathrm{d}\hat{s}\mathrm{d}s}{\|C(\hat{s}) - C(s)\|} \tag{5}$$

where C denotes a curve, and $\mathrm{d}s$ and $\mathrm{d}\hat{s}$ are arc-length measures. Each pair of points on the curve contributes an amount inversely proportional to its distance to the total energy. Note that E_∞ is just the electrostatic potential energy of the charge configuration assuming a three dimensional flux. Unfortunately, it is not hard to show that E_∞ is infinite for every curve. In the next sections, we define energies similar to E_∞ that are finite, and whose resulting gradient flow preserves topology.

3.1. Active Polygons

We define an energy on n-polygons with ordered vertices $\{v_i : i \in \mathbb{Z}_n\}$, $E_p : \mathbb{R}^{2n} \to \mathbb{R}^+$, as

$$E_p(v_0,\ldots,v_{n-1}) = 2\sum_{i\in\mathbb{Z}_n} (|C_i|\ln|C_i| - |C_i|) + \frac{1}{2}\sum_{(i,j)\in\mathbb{Z}_n\times\mathbb{Z}_n, i\neq j} \iint_{C_i\times C_j} \frac{\mathrm{d}\hat{s}\mathrm{d}s}{\|C_i(s) - C_j(\hat{s})\|}. \tag{6}$$

We have used the notation C_i to denote the edge of the polygon connecting v_i to v_{i+1}, and $|C_i|$ to denote the length of C_i. Note that the terms where the integral in (5) diverges, that is, the *self-energies*, $\iint_{C_i\times C_i} \frac{\mathrm{d}\hat{s}\mathrm{d}s}{\|C(\hat{s})-C(s)\|}$, are replaced by the first term of (6). It should be noted that the first term in (6) arises from taking the "finite part" of the self-energies, and discarding the "infinite component". Another way to interpret E_p is

$$E_p(C) = \sum_{i\neq j} E_\infty(C_i, C_j) + \lim_{\epsilon\to 0}\sum_i E^\epsilon_\infty(C_i) + 2L\ln\epsilon$$

where C represents a polygon, L is the total length of C, $E_\infty(C_i,C_j) = \iint_{C_i\times C_j} \frac{\mathrm{d}\hat{s}\mathrm{d}s}{\|C_i(s)-C_i(\hat{s})\|}$, and $E^\epsilon_\infty(C_i) = \iint_{|s-\hat{s}|>\epsilon} \frac{\mathrm{d}\hat{s}\mathrm{d}s}{\|C_i(s)-C_i(\hat{s})\|}$. Thus, we are "subtracting out" the infinity in $E_\infty(C)$ with another infinity $-2L\ln\epsilon$, which diverges at the same rate as the self energies. The result is a finite quantity.

The energy, E_p, is defined on $\mathbb{R}^{2n}$ and hence the gradient of E_p is defined with respect to the inner product on $\mathbb{R}^{2n}$. Therefore, the gradient of E_p, is the vector $\nabla E_p(v_0,\ldots,v_{n-1}) = (\partial E_p/\partial v_k(v_0,\ldots,v_{n-1}))_{k=0}^{n-1}$. It can be shown that

$$F_k = F_k^{\text{self},k-1} + F_k^{\text{self},k} + \sum_{i\in\mathbb{Z}_n\setminus\{k-1\}} F_k^{k-1,i} + \sum_{i\in\mathbb{Z}_n\setminus\{k\}} F_k^{k,i} \tag{7}$$

where $F_k := -\partial E_p/\partial v_k$,

$$F_i^{j,k} = -\frac{\partial}{\partial v_i}\iint_{C_j\times C_k} \frac{\mathrm{d}\hat{s}\mathrm{d}s}{\|C(\hat{s}) - C(s)\|},$$

and

$$F_i^{\text{self},j} = -2\ln|C_j|\frac{v_i - v_j^*}{|C_j|} \text{ for } j = i-1, i.$$

Note that $v_j^* = v_j$ when $j = i-1$, and $v_j^* = v_{j+1}$ when $j = i$. The F's in the above expressions represent "forces"; they get their name from the fact that they are the negative gradient of some term of the energy, E_p. It is important to note, however, that F_k is not the same as the electrostatic force, which is the negative gradient of the *potential integral*, i.e., a single integral. Moreover, F_k is finite for embedded polygons, but the electrostatic force is always infinite. We have derived closed form solutions for F_k; the derivations are lengthy, and the expressions are too long to write in this paper, and therefore, they are given in [21].

We now state the following conjecture that says F_k keeps an active polygon embedded, i.e., the initial topology is preserved, in the presence of image based forces.

Conjecture 1 (Embeddedness of Active Polygon) *Suppose $\{v_0^0, v_1^0, \ldots, v_{n-1}^0\}$ defines an n-polygon embedded in $\mathcal{I}$, $I_k \in C(\mathbb{R}^+, \mathbb{R}^2)$ and I_k satisfies the condition in (2). Consider the n-polygon evolving in time according to the set of ODE defined in (1) with the initial conditions $v_k(0) = v_k^0$ for $k \in \mathbb{Z}_n$, and $R_k := F_k$ where F_k is defined in (7). Then for all $\alpha > 0$, the n-polygon defined according to the set of ODE maintains its initial topology for all $t \in \mathbb{R}^+$.*

It is important to note that Conjecture 1 applies to a finite number of polygons as long as the embeddedness condition is satisfied. The proof of this statement is not trivial since E_p does not necessarily become infinite as the n-polygon approaches a topology change. Note that we label this a conjecture since there are some subtle technical details that we have not verified. The "proof" is found in a technical report [21].

3.2. Active Contours

Let $\mathcal{C}$ denote the set of all twice differentiable embedded curves in $\mathcal{I}$ homeomorphic to the circle. Then we define an energy $E_c : \mathcal{C} \to \mathbb{R}^+$ as

$$E_c(C) = \frac{1}{2} \iint_{C \times C} \left(\frac{1}{\|C(\hat{s}) - C(s)\|} - \frac{1}{d_C(\hat{s}, s)} \right) \mathrm{d}\hat{s}\mathrm{d}s \tag{8}$$

where $d_C(\hat{s}, s)$ denotes geodesic distance, that is, the shortest distance along C from point $C(\hat{s})$ to $C(s)$. To extend this definition to embedded curves that are not necessarily homeomorphic to the circle, simply set $d_C(\hat{s}, s) = +\infty$ if there is no path along the curve C connecting $C(\hat{s})$ to $C(s)$. Since the integral in (8) is the difference of two functions that diverge on the same set, it is natural to ask whether the integral exists. A proof that the integral exists is given in [17]. The energy in (8) is similar to knot energies, which were noted in Section 2, but E_c is not a knot energy since it does not necessarily diverge as the curve approaches self intersection [17]. Hence this energy is not considered in the mathematical literature. We choose to use this energy since the gradient turns out to be easy to compute numerically when the curve is approximated by a polygon. It is important to note that the regularization term, i.e., the second term, in (8) only "cancels out" the infinity of the electrostatic term, i.e., first term, due to points on the curve that are close together in the sense of geodesic distance. The regularization does not affect the asymptotic behavior of the electrostatic term as a curve approaches self intersection. This is because points on the curve that touch during self intersection are far away in the geodesic sense. Finally, we note that the integral of the regularization term does not depend on the geometry of the curve; it only depends on the length of the curve. In fact, one can write formally, $E_c(C) = E_\infty(C) - 2E_\infty(S_{L/2})$ where $S_{L/2}$ is a straight line with length $L/2$ and L is the length of C.

We define the gradient of E_c with respect to the usual geometric L^2 inner product on the space of perturbations of a curve. Defining $B_C(\epsilon, s) = \{C(\hat{s}) : d_C(s, \hat{s}) < \epsilon\}$,

$$\mathcal{E}_\epsilon(s) = \int_{C \setminus B_C(\epsilon,s)} \frac{C(s) - C(\hat{s})}{\|C(s) - C(\hat{s})\|^3} \cdot \mathcal{N}(s)\mathrm{d}\hat{s},$$

where $\mathcal{N}$ is the unit inward normal to C and

$$\mathcal{P}_\epsilon(s) = \int_{C \setminus B_C(\epsilon,s)} \frac{\mathrm{d}\hat{s}}{\|C(s) - C(\hat{s})\|},$$

we state the following proposition, which is proved in a technical report [21].

Proposition 1 (Gradient of E_c) *The gradient of E_c is given by $\nabla E_c(C) = -\mathcal{R}$ where*

$$\mathcal{R}(s) = \lim_{\epsilon \to 0^+} \left[\mathcal{E}_\epsilon(s) + \mathcal{P}_\epsilon(s)\kappa(s) - \ln\left(\frac{L}{2\epsilon}\right)\kappa(s) \right] \mathcal{N}(s), \tag{9}$$

κ denotes the curvature of C, and L denotes the length of C.

The term $\mathcal{E}_\epsilon(s) + \mathcal{P}_\epsilon(s)\kappa(s)$ arises from the electrostatic term of E_c, and the term $\ln(L/2\epsilon)\kappa(s)$ arises from the regularization term. For the sake of intuition, let us ignore the regularization terms in both E_c and $\mathcal{R}$. The energy $E_c(C)$ can then be regarded as the potential energy of a uniform charge distributed along the curve C. The term, $\mathcal{E}_\epsilon(s)$, can be regarded as the projection of the electric field vector of the charge distribution at the point $C(s)$ onto the inward normal of C. The term, $\mathcal{P}_\epsilon(s)$, can be regarded as the electrostatic potential of the charge distribution at the point $C(s)$. Notice that there are two factors that contribute to the energy E_c. One factor is the length of the curve, which is equivalent to the total charge since we are assuming a uniform charge density. The other factor is the "closeness" of points on the curve to other points on the curve. Thus, to reduce energy, the curve should contract, which is equivalent to reducing its charge, in such a way that is consistent with close points moving away from each other due to repulsion of charge. Notice that the term, $\mathcal{P}_\epsilon\kappa\mathcal{N}$, corresponds to contraction of the curve since $\mathcal{P}_\epsilon$ is positive. Since this term is a curvature flow, it keeps the curve smooth and away from irregularities. Repulsion from close points arises from the term, $\mathcal{E}_\epsilon\mathcal{N}$, which is the electrostatic force.

We now state the following conjecture; the conjecture states that $\mathcal{R}$ keeps the active contour embedded in the presence of image based forces.

Conjecture 2 (Embeddedness of Active Contour) *Suppose $C_0 \in C^2([0,1], \mathbb{R})$ defines an embedded curve, $i \in C^2([0,1] \times \mathbb{R}^+, \mathbb{R})$ satisfies the condition in (4), and $\mathcal{R}$ is defined in (9). Consider the curve evolving in time according the PDE defined in (3) with initial condition $C(\cdot, 0) = C_0$. Then for any $\alpha > 0$, the curve defined by the PDE stays embedded for all $t \in \mathbb{R}^+$.*

As in the polygon case, this conjecture applies to multiple curves as long as the embeddedness condition is satisfied. Again, the proof is not trivial since E_c does not become infinite as the curve approaches topology change. We show in [21] that if the curve stays smooth, then the topology of the curve will be preserved. However, we have not shown that the curve remains smooth under this flow and an image based term. We believe, however, that since the

flow contains a positive function times the curvature vector when the limit is evaluated, the curve remains smooth. Hence, we have labeled the statement a conjecture. In the "proof" of the conjecture, it is established that there exists a $p \in [0,1]$ such that $\|\mathcal{R}(p,t)\| \to +\infty$ as a curve approaches topology change. This fact now allows us to define what is meant by a curve being close to topology change. Defining $\tau : \mathcal{C} \to (0, +\infty)$

$$\tau(C) = \frac{1}{\max_{p\in[0,1]} \|\mathcal{R}(p)\|}, \tag{10}$$

we say an embedded curve, C, is close to topology change if $\tau(C)$ is close to zero. A similar measure of closeness to topology change can also be defined for active polygons.

4. Implementation

4.1. Active Polygon Evolution

We implement the polygon evolution by storing the vertices of the evolving polygon in a $n \times 2$ array where n is the number of vertices of the polygon. The vertices are assumed to be ordered so that v_k is adjacent to v_{k+1} for all $k \in \mathbb{Z}_n$. Discretizing the continuous evolution given in (1) yields

$$v_k^{m+1} = v_k^m + \Delta t(I_k^m + \alpha F_k^m)$$

where v_k^m denotes the k^{th} vertex at time m, similarly for the forces F_k^m, I_k^m, and Δt is the step size, which is a small positive number. Note that F_k^m is the sum of n forces that are given in (7). The final expressions for these forces are given in [21]. It is interesting to note that more than one polygon can be evolved using this algorithm, and the presence of F_k guarantees that there will be no self intersections. This same algorithm can be used for a parametric implementation of active contours, except that F_k is replaced with $\mathcal{R}$.

4.2. Active Contour Evolution

We briefly describe an implementation of the contour evolution using level set techniques [18]. That is, to implement the flow in (3), we embed the evolving curve as the zero level set of a scalar function $\Psi : \mathbb{R}^2 \times \mathbb{R}^+ \to \mathbb{R}$ that evolves in time. The evolution of Ψ becomes

$$\Psi_t(x,t) = -\nabla\Psi(x,t) \cdot C_t(x) \quad \text{for } x \in C(t) \tag{11}$$

where C_t is defined in (3), Ψ_t denotes the derivative with respect to the second argument, and $\nabla\Psi$ denotes the gradient with respect to the first argument. The zero level set of Ψ is guaranteed to evolve according to (3). Now, the discrete approximation to (11) on a finite grid using a forward Euler scheme is

$$\Psi_{m+1}(x,y) = \Psi_m(x,y) - \Delta t(\nabla\Psi_m(x,y) \cdot \mathcal{R}_m + \|\nabla\Psi\|_m(x,y)i_m) \tag{12}$$

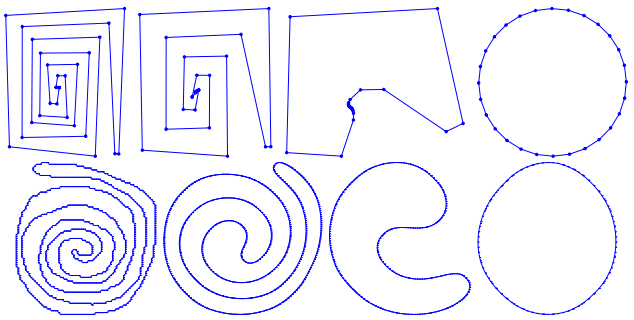

Figure 2. Unwinding of spirals using the proposed topology preserving flow. Spatial scale is shrunk as the evolution progresses.

where the subscript m denotes the time variable. An upwinding differencing scheme is used to estimate $\|\nabla\Psi\|_m$ and $\nabla\Psi_m$, and a central difference scheme is used for a term of the form $\kappa\|\nabla\Psi\|_m$, which is contained in the term $\nabla\Psi_m(x,y) \cdot \mathcal{R}_m$. To efficiently implement (12), we note that Ψ needs to be updated only around a small neighborhood of the zero-level set of Ψ that is called the "narrow band". The quantities i and $\mathcal{R}$ are defined at points in the narrow band to be the same value as at the closest point on the contour to the given point in the narrow band.

The most direct way to compute $\mathcal{R}$ is to find a polygonal estimate of the zero level set at each iteration, and compute $\mathcal{R}$ on this estimate. We have worked out a closed form solution to the integrals in $\mathcal{R}$ for polygonal estimations; these are found in [21]. Another way to calculate $\mathcal{R}$ that may be more efficient and does not require a polygonal estimate of the zero level set is to approximate the integrals of $\mathcal{R}$ with integrals around the entire curve. These integrals can then be written as convolutions over the domain of Ψ, and FFTs can be used to efficiently compute these convolutions. The details are found in [21].

5. Simulations

5.1. Geometric Properties

The top of Fig. 2 shows the evolution of a polygonal spiral under the flow $v_k'(t) = F_k$. Notice that the spiral unravels from the inside by shrinking its inner segments and pushing segments into a small area. Although it looks as if several vertices of the polygon have collapsed to a single point in the evolution, this cannot happen as the "proof" of Conjecture 1 shows [21]. The polygon then becomes convex, and finally converges to a regular polygon. We believe that any polygon converges to a regular polygon under this topology preserving flow, but this has not been proved. Therefore, this flow can also be used as a regularity term in addition to preserving topology for segmentations. The bottom row of Fig. 2 shows the evolution of a spiral evolving

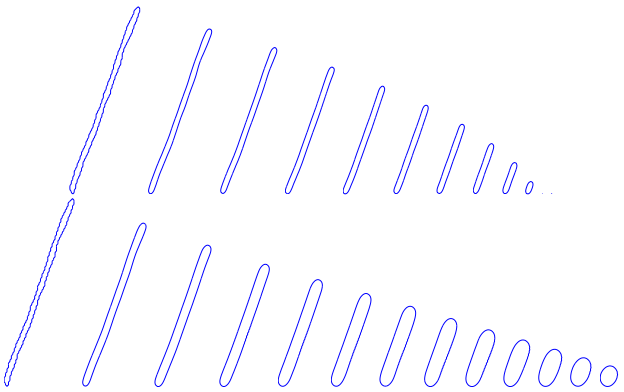

Figure 3. Illustration of a difference between curvature flow (top) and proposed flow (bottom).

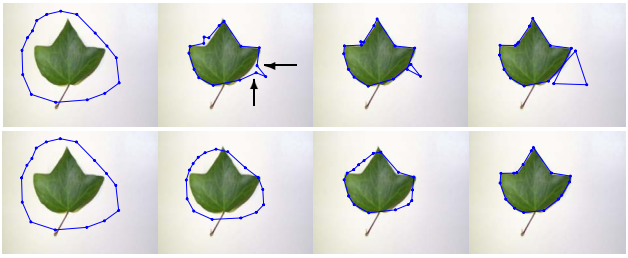

Figure 4. Simple leaf segmentation without (top) and with (bottom) proposed flow.

under $C_t = \mathcal{R}$. The spiral eventually becomes convex, becomes circular, and shrinks to a configuration that is not representable with the given resolution of the level set function. The behavior of this flow, as witnessed through this simulation, shows some similarities to curvature flow. In particular, the proposed topology preserving flow has smoothness properties like curvature flow. Indeed in [21], we prove that a circle, under our flow, shrinks in finite time to a point. Also, it has been shown in [1] that E_c is minimized by a circle among curves having a constant perimeter. However, as shown in Fig. 3, the topology preserving flow also has different properties than curvature flow. In this figure, the evolution of a thin, long curve is shown. The top of the figure shows the evolution under curvature flow, and the bottom of the figure shows the evolution under the proposed flow. Notice that the curve on the bottom of the figure becomes thicker as parallel sides are pushed apart. This is due to the term $\mathcal{E}_\epsilon \mathcal{N}$. Since these parallel sides have nearly zero curvature, curvature flow does not push the sides apart.

5.2. Image Segmentations

In all the following image segmentations, we have used the Chan-Vese flow [4] as the image based term. The Chan-Vese flow, in summary, moves a contour or polygon to separate an image into two regions that are piecewise constant. Results of segmentation of a simple leaf image with an active polygon are shown in Fig. 4. The result of the running the Chan-Vese flow without the proposed topology preserving flow is shown on the top row of Fig. 4. Notice that a topology change occurs between the second and third image. From the nature of the Chan-Vese flow, the vertices indicated by the arrows in Fig. 4 will move the polygon toward self intersection. This is because the vertices will move in the direction that reduces the white area as fast as possible; clearly, the direction of the vertices that decreases white area fastest moves the polygon toward self intersection. After self intersection, the normal vectors become flipped at the indicated vertices, and the flow moves in the wrong direction. Since there is no way to consistently define a normal vector field when the polygon is no longer embedded, this problem cannot be corrected. The bottom row of Fig. 4 shows snapshots of the evolution of Chan-Vese flow weighted 98% and the topology preserving flow weighted 2%. Notice the continuous motion of the polygon to keep the polygon away from self intersection. In addition, the polygon is more "regular" during the evolution than the polygon that results without using the topology preserving flow.

The next simulations are segmentations with active contours. Figure 5 shows the results of segmentation of an image with two closely spaced bones with no topology preservation, topology preservation (Han [10]), and more-than-topology preservation, i.e., the proposed method. The top rows is the result with a curvature prior; the curvature is weighted 50% to compensate for the noise. As can be seen, the two contours merge across the thin gap between the two bones. This merging is due to the nature of the image and Chan-Vese flow, and not a step size problem. The middle row shows the result of the topology preserving method of Han [10] with curvature weighted 50%. The final row shows the result with our proposed more-than-topology-preserving flow weighted 27% and the remaining percent only the image based term. We wish to comment that the topology preservation method of Han simply stops the evolution at points of the contour where a topology change will occur as result of updating the level set function. Often times the contour is stopped in an arbitrary location relative to the image features, and is stopped at a distance based on the grid spacing of the level set function. This phenomena is illustrated in Fig. 6, which provides a zoom of the region separating the two bones. Our method pushes the contour to attract relevant image features, and does more than just topology preservation.

Figure 7 shows a segmentation of a simple image of two circles connected by a thin line with active contours to fur-

Proceedings of the Tenth IEEE International Conference on Computer Vision (ICCV'05)
1550-5499/05 $20.00 © 2005 **IEEE**

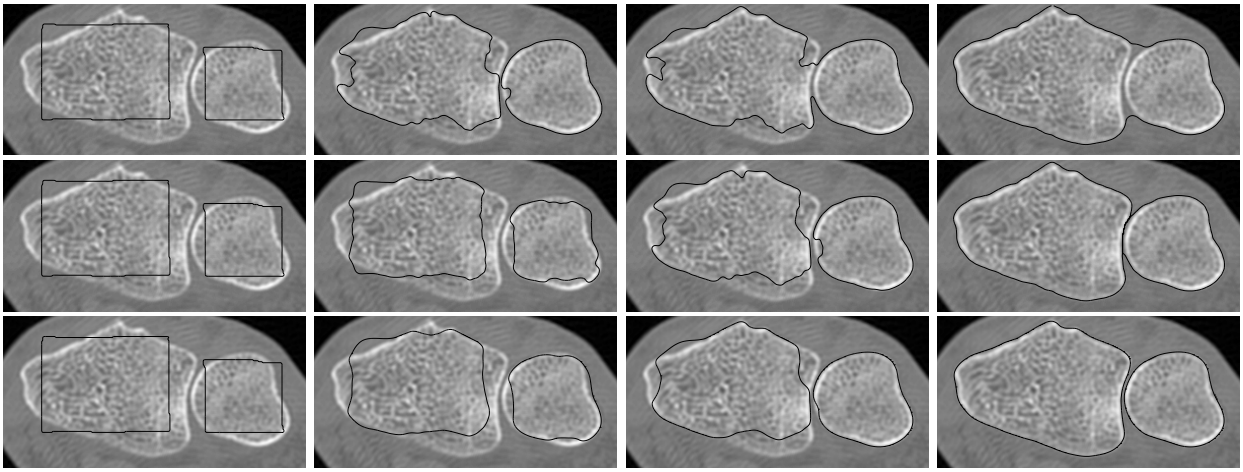

Figure 5. Segmentation of bones CT image with no topology preservation (top), with topology preservation of Han (middle), and with more-than-topology preservation (bottom). (Image courtesy of Ben Kimia.)

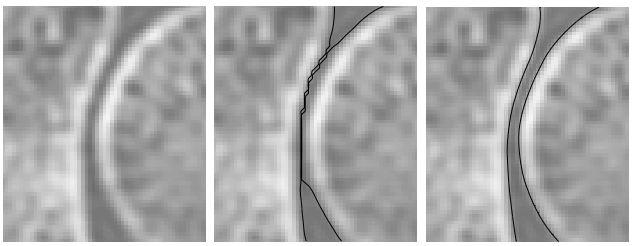

Figure 6. Gap between bones with contours overlaid. Results of no topology preservation, topology preservation of Han, and more-than-topology preservation.

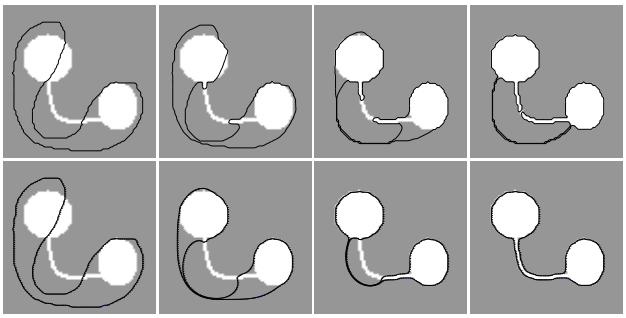

Figure 7. Incorrect segmentation by topology preservation method of Han [10] (top), and correct segmentation by the proposed more-than-topology preserving flow.

ther illustrate the degeneracies of the method of Han. The top row shows the result of the topology preserving level set method of Han [10], and the bottom row shows the results of the proposed method. Note that we have used a curvature force (weighted 10%) in the method of Han to keep the curve smooth. The method of Han results in a "degenerate" curve as shown in the figure. The resulting curve is close to topology change. Although the topology is correct, the segmentation is incorrect. One may argue that weighting the curvature high enough in the method of Han will correct this problem. However, weighting the curvature just enough, produces a flow that looks like curvature flow, and fails to even capture the circles in the image. The bottom row of Fig. 7 shows the result of segmentation with Chan-Vese flow weighed 96% and the proposed more-than-topology-preserving flow weighted 4%. The segmentation with the proposed method does not have the problem with that of Han's method. The curve repels from itself in a continuous manner as it becomes close to self intersection. The curve is then pushed in the right direction to capture the thin strip as the thin strip slowly becomes detected.

6. Conclusion

In summary, we have presented a novel method for enforcing a prior assumption on the topology of objects to be detected from an image. This method is a geometric flow that can be added to existing image based evolutions of active polygons or contours. We have demonstrated that our flow does more than mere topology preservation, and that our method gradually and continuously preserves topology. We presented possible numerical schemes for implementing the topology preserving flow for both active contours and

active polygons. Experimental results were shown to illustrate the geometrical properties of the topology preserving flows. In particular, it was shown that the flows had regularizing properties like the curve shortening flow. Experiments involving the use of the topology preserving flow in segmentations of real images was shown, and compared to segmentations not using the proposed topology preserving flow. We also compared our method to the method of Han [10], and showed how our method corrected some undesirable features of Han's method.

The energies defined in this paper naturally extend to surfaces, and therefore, future work will be to consider extending this topology preserving flow to surfaces. Topology preservation for surfaces is an interesting problem since the common method to smooth surfaces, mean curvature, works to change the topology of a surface in the non-convex case.

7. Acknowledgments

We wish to thank Jeremy Jackson for the implementation of Han's method and Ben Kimia for providing the bone image. We also thank an anonymous reviewer for pointing out some relevant references.

References

[1] A. Abrams, J. Cantarella, J. Fu, M. Ghomi, and R. Howard. Circles minimize most knot energies. *Topology*, (42):381–394, 2003.

[2] A. M. Bruckstein, G. Sapiro, and D. Shaked. Evolutions of planar polygons. *Int. J. of Pattern Recognition and Artificial Intelligence*, 9:991–1014, 1995.

[3] V. Caselles, R. Kimmel, and G. Sapiro. Geodesic active contours. In *Proceedings of the IEEE Int. Conf. on Computer Vision*, pages 694–699, Cambridge, MA, USA, June 1995.

[4] T. Chan and L. Vese. Active contours without edges. *IEEE Transactions on Image Processing*, 10(2):266–277, February 2001.

[5] H. Chang and D. Valentino. Medical image segmentation using a simulated charged fluid. In *Proceedings of SPIE*, volume 5370, pages 494–505, 2004.

[6] M. H. Freedman, Z. X. He, and Z. Wang. Mobius energy of knots and unknots. *Annals of Mathematics*, 139(1):1–50, 1994.

[7] M. Gage and R. S. Hamilton. The heat equation shrinking convex plane curves. *Journal of Differential Geometry*, (23):69–96, 1986.

[8] M. Grayson. The heat equation shrinks embedded planes curves to round points. *J. Differential Geometry*, (26):285–314, 1987.

[9] X. Han, C. Xu, and J. Prince. Topology preserving deformable model using level sets. In *Proceedings of IEEE Conference on Computer Vision and Pattern Recognition*, pages 765–770, Hawaii, December 2001.

[10] X. Han, C. Xu, and J. Prince. A topology preserving level set method for geometric deformable models. *IEEE Transactions on Pattern Analysis and Machine Intelligence*, 25(6):755–768, June 2003.

[11] G. Hermosillo, O. Faugeras, and J. Gomes. Unfolding the cerebral cortex using level set methods. In *Second Int'l Conf. Scale-Space Theories in Computer Vision*, pages 58–69, 1999.

[12] J. Jackson, A. Yezzi, W. Wallace, and M. Bear. Segmentation of coarse and fine scale features using multi-scale diffusion and mumford-shah. In L. Griffin and M. Lillholm, editors, *Scale-Space*, pages 615–624, 2003.

[13] A. Jalba, M. Wilkinson, and J. Roerdink. Cpm: A deformable mode for shape recovery and segmentation based on charged particles. *IEEE Transactions on Pattern Analysis and Machine Intelligence*, 26(10):1320–1335, 2004.

[14] M. Kass, A. Witkin, and D. Terzopoulos. Snakes: Active contour models. *International Journal of Computer Vision*, 1:321–331, 1987.

[15] S. Kichenassamy, A. Kumar, P. Olver, A. Tannenbaum, and A. Yezzi. Gradient flows and geometric active contour models. In *Proceedings of the IEEE Int. Conf. on Computer Vision*, pages 810–815, 1995.

[16] D. Mumford and J. Shah. Optimal approximations by piecewise smooth functions and associated variational problems. *Comm. Pure Appl. Math.*, 42:577–685, 1989.

[17] J. O'Hara. Energy of a knot. *Topology*, 30(2):241–247, 1991.

[18] S. Osher and J. Sethian. Fronts propagating with curvature-dependent speed: algorithms based on the Hamilton-Jacobi equations. *Journal of Computational Physics*, 79:12–49, 1988.

[19] N. Paragios and R. Deriche. Geodesic active regions and level set methods for supervised texture segmentation. *International Journal of Computer Vision*, 46(3):223, 2002.

[20] M. Rochery, I. Jermyn, and J. Zerubia. Higher order active contours and their application to the detection of line networks in satellite imagery. In *IEEE Workshop on VLSM*, October 2003.

[21] G. Sundaramoorthi and A. Yezzi. Global geometric flows for topology preservation of active contours and polygons. Technical report, Georgia Institute of Technology, `http://users.ece.gatech.edu/~ayezzi`, 2005.

[22] G. Unal, A. Yezzi, and H. Krim. Unsupervised texture segmentation by information-theoretic active polygons. *Int. J. Computer Vision*, 62(3):199–220, 2005.

[23] A. Yezzi, A. Tsai, and A. Willsky. A statistical approach to snakes for bimodal and trimodal imagery. In *International Conference on Computer Vision*, pages 898–903, October 1999.